ICARUS **122,** 193–199 (1996)
ARTICLE NO. 0118

# Crater-Centered Laccoliths on the Moon: Modeling Intrusion Depth and Magmatic Pressure at the Crater Taruntius

R. W. WICHMAN

*Department of Space Studies, University of North Dakota, Grand Forks, North Dakota 58202-9008*
E-mail: wichman@plains.nodak.edu

AND

P. H. SCHULTZ

*Department of Geological Sciences, Brown University, Providence, Rhode Island 02912*

Received June 23, 1995; revised December 18, 1995

**Many floor-fractured craters on the Moon show surface deformation like that seen over terrestrial laccoliths. Consequently, terrestrial laccoliths provide one model for such crater modification. This model directly relates surface deformation to the growth of a shallow, crater-centered intrusion, and it estimates intrusion size and magma pressure. It also yields a minimum estimate for intrusion depth. Maximum intrusion depths cannot be directly constrained, but a range of likely intrusion depths can be derived with additional assumptions. When the model is applied to the crater Taruntius, the surface record indicates an intrusion ~30 km across and 1900 m thick. The calculated excess magma pressure is ~9 MPa (90 bar), and the estimated intrusion depths range from ~1 to ~5 km. If magma pressure reflects a hydrostatic magma column beneath Taruntius, these values suggest a total magma column length of ~65 km during crater modification.** 

## INTRODUCTION

Over 200 craters on the Moon contain distinctive fracture patterns in and around their crater floors. These craters are often much shallower than pristine craters of the same size, are preferentially located near the lunar maria, and repeatedly contain minor volcanic units (Schultz 1972, 1976, Young 1972, Whitford-Stark 1974). In addition, these craters apparently record a systematic process of endogenic crater modification (Schultz 1976). In the least modified craters, fracturing and minor volcanism primarily occur in the central crater floor, and crater depths are essentially unchanged. At higher levels of modification, however, later failure and volcanism are concentrated into a ring near the edge of the crater floor, and floor uplift begins to reduce the crater depth. In many cases, this produces an exceptionally shallow crater with a moat-like depression around the crater floor (Schultz 1976). Rarely, in cases of extreme crater modification (e.g., Gassendi), deformation can extend beyond the crater rim to form another annular trough surrounding a narrowed, ridge-like crater rim (Schultz 1976).

This sequence of progressive crater floor uplift can be attributed to both a viscous relaxation of crater topography (e.g., Danes 1965, Hall *et al.* 1981) and the emplacement of crater-centered intrusions (e.g., Schultz 1972, 1976, Brennan 1975). However, several observations appear to favor the igneous intrusion mechanism. In particular, the frequency of crater-centered volcanism, the equilibration of uplifted crater floors with nearby mare levels, and the selectivity of crater modification in some regions are all more consistent with igneous intrusions than with viscous relaxation (Schultz 1976). Further, the relative degree of crater shallowing is size dependent in some regions: small craters show proportionally greater floor uplifts than larger floor-fractured craters (Wichman and Schultz 1995). Such behavior contrasts sharply with the predicted effects of viscous relaxation, where floor uplift preferentially removes the longest topographic wavelengths before affecting smaller craters within a region.

Although igneous intrusion models qualitatively explain many elements seen in floor-fractured craters, previous studies have provided few quantitative tests for these modification models. Consequently, we have worked to develop a more quantitative model for igneous crater modification (Wichman 1993). This model links the apparent sequence of crater floor fracturing to the emplacement and growth of shallow, crater-centered laccoliths (Fig. 1). Failure of the central crater floor is ascribed to early flexure over the intrusion, while moat formation and the majority of floor uplift are attributed to a later stage of piston-like intrusion



0019-1035/96 $18.00

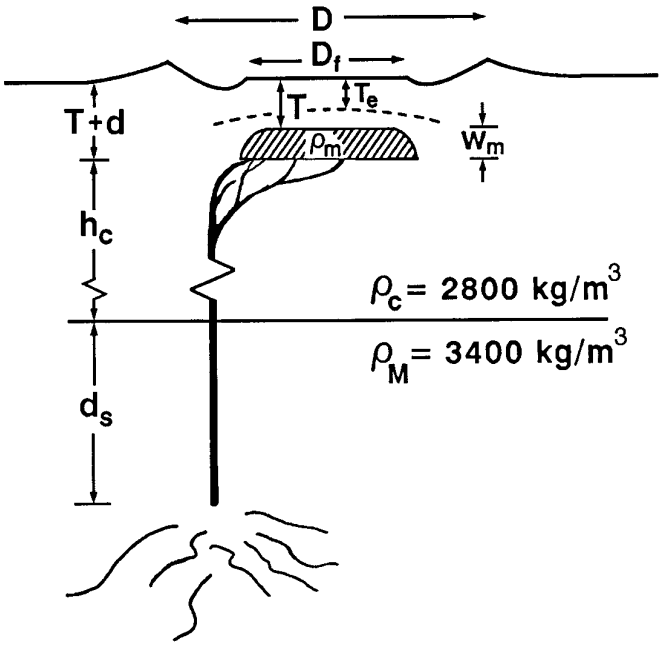


**FIG. 1.** Schematic diagram for crater modification by a laccolith. $D$ is the crater diameter; $D_f$ is the crater floor diameter and the approximate diameter of the intrusion. $w_m$ is the thickness of the intrusion and the extent of floor uplift; in this example, floor uplift is equal to the initial apparent crater depth ($d$). $T$ is the thickness of the uplifted floor block, and $T_e$ represents the effective flexural thickness of the floor plate during uplift. Beneath the intrusion, $h_c$ denotes the length of the crustal magma column, and $d_s$ measures the depth these magmas extend beneath the Moho. For the hydrostatic calculations in the text, $\rho_m$ is the magma density (~2900 kg/m$^3$), $\rho_c$ is the crustal density, and $\rho_M$ is the mantle density.

growth. Modification is presumed to be independent of the impact event, and the intrusions are assumed to form within breccia-defined zones of neutral buoyancy. Thus, while such intrusions should reflect local magmatic conditions (Wichman and Schultz 1995), crater structures may influence both the dimensions and the locations of the modeled intrusions (Wichman 1993).

A preliminary version of this model is presented in Schultz (1976), but that study places only loose constraints on the depth and other attributes of the inferred intrusions. More detailed constraints are developed here by linking the Schultz (1976) paradigm with terrestrial models for laccolith growth (Wichman 1993, Wichman and Schultz 1995). Specifically, surface deformation over terrestrial laccoliths is related to intrusion dimensions, magma pressure, and an effective intrusion depth (Johnson and Pollard 1973, Pollard and Johnson 1973). Thus, similar intrusion parameters can be estimated from the deformation over a crater-centered laccolith.

This paper describes the quantitative elements of our crater modification model. First, we review the theoretical equations which describe deformation at terrestrial laccoliths. Then, we specify the assumptions needed to apply these relations to lunar crater modification. Last, we apply the model to the lunar crater Taruntius to illustrate a model calculation for magmatic pressure, intrusion depth, and regional magma column length.

## TERRESTRIAL LACCOLITHS

Laccoliths are tabular or domical intrusions that evolve from sill-like forms by lifting the overlying strata (Gilbert 1877, Corry 1988). Their inflation, however, depends on the style of nearby crustal failure, and it varies with time. Thus, three distinct stages of laccolith formation are recognized (Johnson and Pollard 1973, Corry 1988): (1) initial growth of a thin sill-like unit, (2) vertical growth by magmatically induced flexure, and (3) piston-like uplift of a fault-bounded block. Since sill growth occurs by localized brecciation and failure at the intrusion edge (Pollard and Johnson 1973), this discussion focuses on the later stages of vertical intrusion growth, which are more likely to produce surface deformation.

### *The Deformation Model*

From the analysis of Pollard and Johnson (1973), three variables control the initiation of vertical intrusion growth: magma pressure, intrusion size, and crustal strength. Due to the effects of lithostatic pressure ($P_L$), however, the magma pressure ($P_d$) driving deformation around an intrusion is only a fraction of the total magma pressure ($P_m$) in that intrusion (Gilbert 1877, Johnson and Pollard 1973):

$$P_d = P_m - P_L. \tag{1}$$

During lateral sill growth, this driving pressure causes failure only at geometric stress concentrations near the sill edge (Pollard and Johnson 1973). As the sill expands, however, the net upward force on the overburden grows in proportion to the (increasing) intrusion floor size (Gilbert 1877). When this load finally exceeds the rigid strength of the overburden, the later stages of laccolith growth by crustal uplift begin (Pollard and Johnson 1973, Corry 1988).

For the second stage of laccolith growth, deformation over the intrusion is approximated by flexure of the overburden as a layered sequence of elastic plates (Pollard and Johnson 1973). Under these conditions, the maximum uplift at any given time is related to $P_d$, and to the effective elastic thickness of the overburden, $T_e$, by

$$P_d = \frac{5.33 w_m B T_e^3}{a^4}, \tag{2}$$

where $w_m$ is the thickness of the intrusion, $a$ is the radius of an axisymmetric intrusion, and $B$ is the elastic modulus

of the surrounding country rock (Pollard and Johnson 1973). When uplift is limited, brittle failure should be minor and may primarily occur at the surface. As uplift continues, however, two responses become possible. First, if crustal failure is primarily ductile in character, flexure can continue throughout intrusion growth (Corry 1988) leaving the final intrusion bounded by an arcuate, monoclinal fold. Alternatively, if bending causes cracking and failure near the intrusion edge, deep-seated failure can separate the uplifted section from the rest of the crust (Pollard and Johnson 1973), thereby initiating uplift of a fault-bounded roof block.

For the third stage of block uplift, Gilbert (1877) postulated that vertical intrusion growth is resisted primarily by shear along the bounding normal faults. Such resistance seems to be fairly small, however, as such uplifts typically show little internal deformation on Earth. Further, because the integrated driving pressure in the intrusion must exceed fault drag for uplift to occur, there is little constraint on the magmatic conditions during this stage of uplift. Still, if the uplifted block is totally supported by magma at the end of uplift, then the final intrusion thickness should reflect the magma pressure in that laccolith through the equation (Pollard and Johnson 1973)

$$P_d = w_m \left( \frac{2k}{a} + \gamma_m \right). \quad (3)$$

In this equation, $k$ is the magma yield strength, and $\gamma_m$ represents the unit magma weight in the intrusion.

In combination, Eqs. (2) and (3) provide a fairly simple basis for modeling the sequence and conditions of deformation over a terrestrial laccolith (Pollard and Johnson 1973). Given the intrusion size and thickness, Eq. (3) constrains the magmatic pressure, $P_d$, and this value is then inserted into Eq. (2) to estimate the effective overburden thickness under various conditions.

### *Application to Lunar Craters*

Although Eqs. (2) and (3) relate surface uplift to subsurface intrusion parameters, their application to lunar intrusions is complicated at present by a lack of field data. On Earth, such data generally constrain the model values for intrusion dimensions and local material properties (Johnson and Pollard 1973, Jackson and Pollard 1988). On the Moon, however, comparable constraints are limited or not available. Consequently, an extension of Eqs. (2) and (3) to crater-centered intrusions on the Moon requires assumptions characterizing (i) the material properties of lunar magmas and impact breccias, and (ii) the relation of intrusion dimensions to deformation at the surface.

**TABLE I**
**Material Constants and Related Parameters**

| Symbol | Definition | Assumed value |
|---|---|---|
| $E_m$ | Young's Modulus (basalt) | $7.0 \times 10^{10}$ Pa |
| $\nu$ | Poisson's Ratio | 0.25 |
| $B_m$ | Elastic modulus of country rock = $E/(1 - \nu^2)$ | $7.47 \times 10^{10}$ Pa |
| $k$ | Magma yield strength | $10^4$ N/m$^2$ |
| $g$ | Lunar gravitational acceleration | 1.62 m/s$^2$ |
| $\rho_m$ | Magma density | 2900 kg/m$^3$ |
| $\gamma_m$ | Unit magma weight ($=\rho_m$ g) | 4700 kg/m$^2$s$^2$ |

For the needed material constants (Table I), we assume here that flexure over a crater-centered intrusion is dominated by the response of a coherent impact melt unit. Therefore, the elastic modulus $B$ in Eq. (2) is assigned an average value derived for terrestrial basalts. We also assume that the intrusion magmas are typical mare basalts. Thus, the magma densities derived for sampled mare basalts (Solomon 1975) are used to estimate unit magma weight ($\gamma_m$), while magma yield strength ($k$) is equated to a representative value for terrestrial diorites (Pollard and Johnson 1973). Although analyses of lava flow morphology in Mare Imbrium suggest lunar yield strengths significantly below our assumed value (Hulme 1974, Moore and Schaber 1975), correction of these values for an apparent dependence on regional slope (Moore *et al.* 1978) supports such a correlation. Moreover, since yield strength is normalized by intrusion size in Eq. (3), this term is negligible for lunar intrusions over ~10 km in diameter.

For intrusion dimensions, the size and thickness of most laccoliths on Earth are derived from surface exposures and/or gravity analyses. Erosion is limited on the Moon, however, and our present gravity data cannot characterize gravity signatures in craters less than ~100 km in diameter (Schultz 1976). Consequently, we estimate intrusion size and thickness from the observed crater modifications. First, since horizontal intrusion growth is nearly negligible after vertical uplift begins (Johnson and Pollard 1973, Corry, 1988), the similarity of lunar floor plate uplifts to terrestrial punched laccoliths suggests that these floor plates approximate the size of the underlying intrusions (Fig. 1). Similarly, since pristine crater depths are a well-defined function of crater size (Pike 1980), the change in crater depth due to uplift provides a simple estimate for intrusion thickness. Greater intrusion thicknesses can develop if ductile failure thins the uplifted crater floors, but there is little evidence for such failure on the Moon. Both the limited failure inside crater floor plates and the correlation of floor plate sizes to initial crater floor dimensions (Wichman 1993) suggest that extension, and therefore thinning, of the floor plate is minimal in lunar craters.

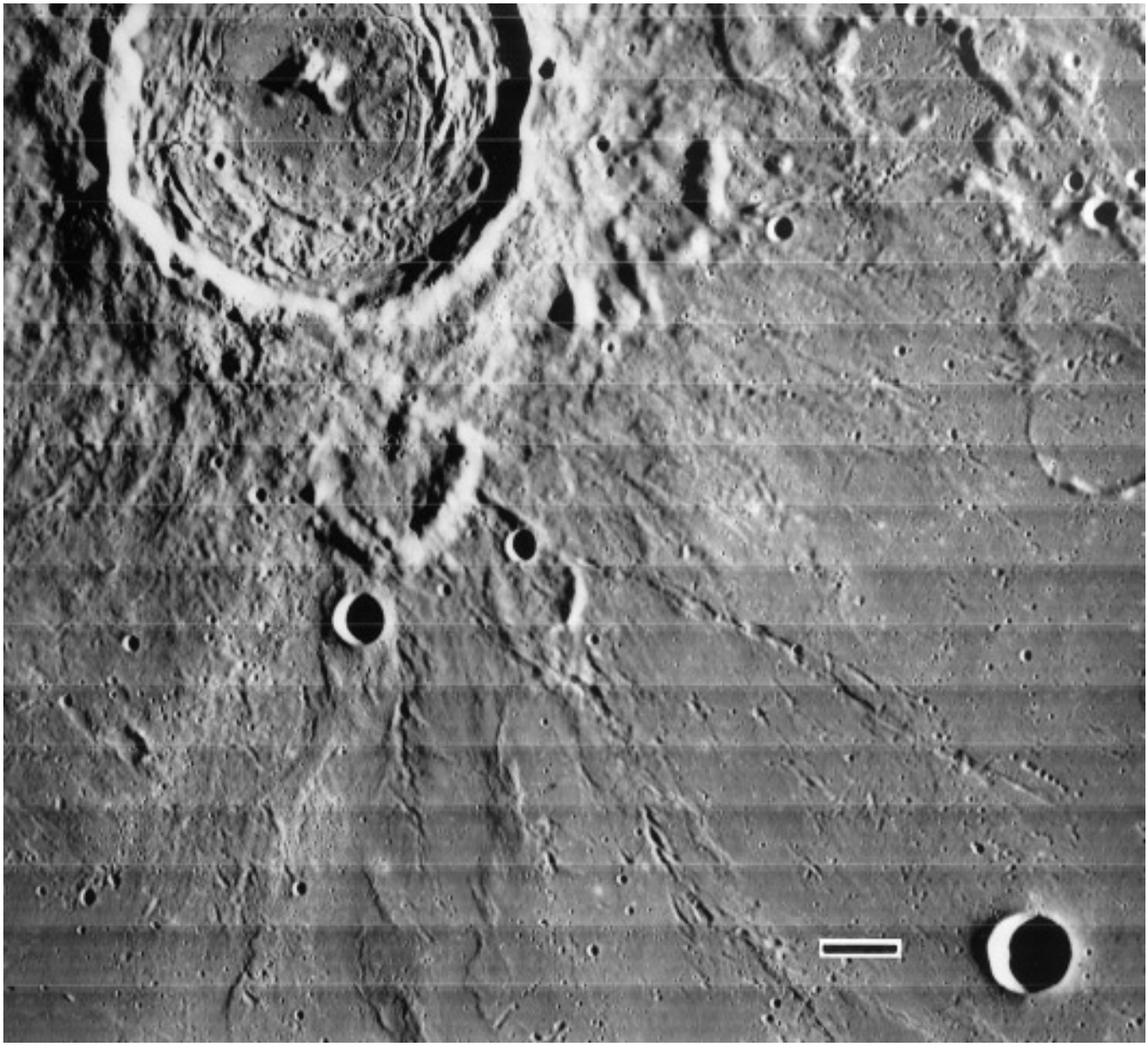

**FIG. 2.** The crater Taruntius, located between Mare Tranquillitatis and Mare Fecunditatis. Crater diameter is 56 km; scale bar is 11 km. Note both the fresh ejecta features outside the crater and the smooth floor region bounded by a pronounced ring of concentric failure.

## IMPLICATIONS FOR TARUNTIUS

The crater Taruntius is ~56 km in diameter. Outside the crater rim, its ejecta and secondary impact features are nearly pristine (Fig. 2). Inside the crater, however, is a prominent ring of concentric ridges and subdued fractures. These surround a smooth, uplifted central floor (like that in Fig. 1) which is ~28–30 km wide. The innermost, floor-bounding scarp/ridge has a diameter of ~30–32 km. At present, the apparent crater depth is only ~400 m, whereas the expected depth for craters of this size is ~2300 m (Pike 1980). The preserved crater rim heights (~900–1500 m), however, are comparable to the predicted, pristine crater rim height (~1200 m; Pike 1980). Thus, the change in depth at Taruntius is primarily attributed to floor uplift and not to rim degradation or crater filling.

### *Basic Model*

Fitting our laccolith model to these observations, we assume that the intrusion radius, $a$, is 15 km and that the final intrusion thickness, $w_{\mathrm{m}}^{\mathrm{f}}$, is 1900 m. For the material

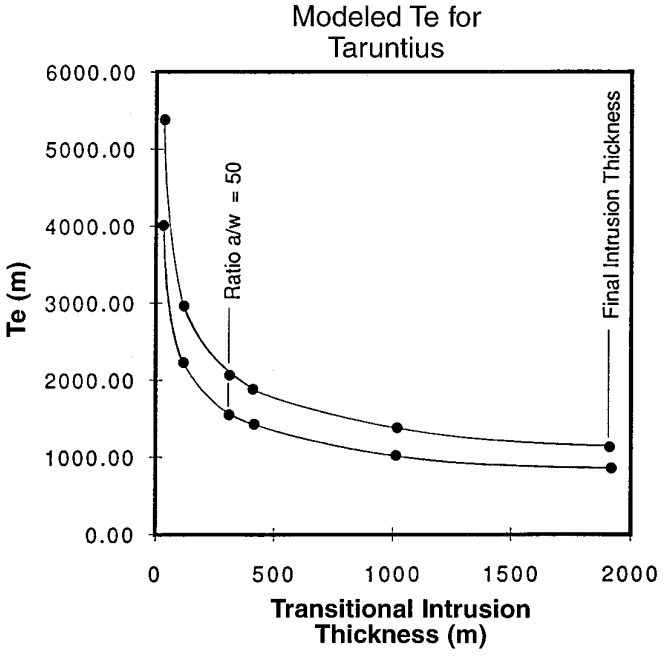


**FIG. 3.** Relation of inferred plate thickness at Taruntius to intrusion thickness at the transition from magmatically induced flexure to block uplift. The lower curve shows calculated plate thicknesses assuming an elastic modulus appropriate for basalt; the upper curve shows the effect of a weaker elastic modulus ($B_{br} = 3.2 \times 10^{10}$ Pa). Both curves assume an intrusion radius of 15 km and a magmatic pressure of 89 bar.

constants in Table 1, therefore, Eq. (3) indicates a final magma driving pressure of 8.9 MPa (89 bar) for the inferred intrusion. Equation (2) then provides a minimum value for both the thickness of the uplifted crater floor and the intrusion depth. Specifically, if we assume that the final $P_d$ is similar to magma pressures during the earlier stages of uplift, Eq. (2) relates effective floor plate thickness to intrusion thickness and intrusion radius during flexurally controlled intrusion growth.

Intrusion thicknesses during this stage are unknown, but the $T_e$ values can still be modeled by considering the likely range of transitional intrusion thicknesses ($w_m^t$) at the end of flexural uplift (Fig. 3). For instance, since $T_e$ is inversely related to intrusion thickness, setting $w_m^t = w_m^f$ yields the smallest possible value for $T_e$. For Taruntius, this implies a minimum $T_e$ of ~840 m. Alternatively, setting $w_m^t$ equal to the initial sill thickness gives a maximum value for $T_e$ (Pollard and Johnson 1973). Johnson and Pollard (1973) show that sill-like intrusions of Bingham rheology have a maximum halflength to thickness ratio that is proportional to both magma pressure and magma yield strength,

$$\frac{a_{max}}{w_m} = \frac{P_d}{k}. \quad (4)$$

Therefore, for the estimated intrusion radius and the assumed magma yield strength, the minimum thickness of a crater-centered sill at Taruntius is ~17 m and the associated value of $T_e$ is ~4050 m.

Both of these thickness estimates are a little extreme. On the one hand, the flat, undeformed central floor at Taruntius suggests that most of the observed uplift is not a product of flexure. On the other hand, an intrusion 30 km wide and 17 m thick seems unlikely to produce the bending strains needed to initiate fault-bounded floor uplift. Consequently, an intermediate model may be more appropriate. Since terrestrial laccoliths in Utah apparently formed from sills with halflength/thickness ratios of ~50 (Pollard and Johnson 1973), we suggest that 300 m is a reasonable estimate for sill thickness at the onset of flexure. Allowing some small amount of flexure (~100 m) before the start of block uplift, $w_m^t$ then becomes ~400 m and the modeled value for $T_e$ at Taruntius is ~1400 m (Fig. 3).

### *Modeling Intrusion Depth*

These values for $T_e$ are minimum estimates for the uplifted overburden thickness. Thus, they also constrain the depth of an intrusion beneath the crater floor. Where Eq. (2) assumes the flexure of a single elastic layer, however, the effective thickness of a layered section can be much smaller than its true stratigraphic thickness (Pollard and Johnson 1973). Therefore, since impact melt units, fallback ejecta layers and deeper breccias may produce a crudely layered crater floor stratigraphy (Schultz 1976, Dence *et al.* 1977), the $T_e$ values in our example provide only minimum estimates for the intrusion depth.

Similar constraints on the maximum intrusion depth cannot be directly derived from the model equations. Nevertheless, a range of greater intrusion depths can be modeled as a function of floor stratigraphy. Specifically, for a stack of decoupled stratigraphic layers (Pollard and Johnson 1973),

$$T_e^3 = \sum_{i=1}^{n} \frac{B_i}{B_e} t_i^3, \quad (5)$$

where $n$ is the number of layers, $B_e$ is the elastic modulus used to calculate $T_e$, $B_i$ is the elastic modulus of each layer, and $t_i$ is the thickness of each layer. For the small laccolith at Buckhorn Ridge, Utah, this equation yields an effective flexural thickness that is approximately one-seventh of the actual overburden thickness (~2100 m; Pollard and Johnson 1973). (Note: This equation maximizes the contrast between stratigraphic thickness and $T_e$, and thus yields the greatest endmember model for intrusion depth.)

Although the subfloor stratigraphy in lunar craters is poorly known, rudimentary models for intrusion depth can thus be derived by considering the origin of the shallow crater floor. For instance, where sedimentary sections on the Earth contain many distinct, fairly thin layers, the lack

**TABLE II**
**Theoretical Inversions for Intrusion Depth at Taruntius[a]**

Model 1[b]

| Case | Layers ($n$) | $t_i$ (km) | $T = nt_i$ (km) |
|---|---|---|---|
| A | 1 | $T_e$ | 1.41 |
| B | 2 | 1.12 | 2.24 |
| C | 3 | 0.98 | 2.93 |
| D | 5 | 0.82 | 4.12 |

Model 2[c]

| Case | Layers ($n$) | $t_m$ (m) | $t_{br}$ (km) | $T$ (km) |
|---|---|---|---|---|
| E | 2 | 500 | 1.84 | 2.34 |
| F | 3 | 500 | 1.46 | 3.42 |
| G | 5 | 500 | 1.16 | 5.14 |

[a] All cases assume transitional $w_m = 400$ m, $T_e = 1.96$ km, and $B_m = 7.47 \times 10^{10}$ Pa.

[b] Assumes floor plate deforms as stack of $n$ free-slipping, equivalent layers.

[c] Assumes floor plate divided into a single coherent impact melt layer ($t_m$) and $n - 1$ free-slipping breccia layers of weaker elastic modulus ($B_{br} = 3.2 \times 10^{10}$ Pa).

of sedimentation on the Moon should preclude such finely layered sections. Moreover, the combination of excavation, brecciation, and central peak uplift during crater formation should effectively disrupt any pre-existing, near-surface layers beneath the crater floor. Consequently, if only the distribution of impact melts and breccias controls layering in the crater floor, crater floor stratigraphies should contain fewer, thicker layers than the sedimentary sections hosting most laccoliths on Earth.

This interpretation suggests that $N$, the number of uplifted layers in any crater floor plate, is small and that a range of likely intrusion depths can be derived by assuming different values for $N$. Table II summarizes two such model depth ranges where $N \leq 5$. The first of these depth ranges (Cases A–D) simply assumes that the floor plate contains $n$ layers of equal thickness $t$ and constant elastic modulus $B$. Consequently, the total plate thickness, $T$, is an exponential function of $n$, and the derived intrusion depths range from $T_e$ (1.4 km) up to ~4.1 km.

The second depth range (Cases E–G) uses a potentially more realistic model. In the simplest case ($n = 2$), this model divides deformation between a thin, coherent impact melt sheet and a thicker breccia layer at depth. Based on measured or inferred impact melt thicknesses on Earth (Grieve and Cintala 1992), we fix the melt thickness in Taruntius at ~500 m. We also assign the breccia a weaker elastic modulus ($B_{br} \sim 3.2 \times 10^{10}$ Pa), comparable to many sedimentary rocks on Earth. Because both impact heating and disseminated impact melts should allow some welding of these breccias after impact, the inferred coherence of this layer is not unreasonable. Nevertheless, changes in the degree of either fracturing or welding as a function of depth may allow the breccias to respond as multiple layers. For these cases in Table II (F, G), the breccia layers are assumed to be of equal thickness. Again, overall plate thickness is an exponential function of $n$, and the derived intrusion depths range from ~2.3 to 5.1 km (Table II).

### *Regional Magmatism*

Magma pressures in a laccolith depend directly on the pressure in its feeder dike (Johnson and Pollard 1973). Thus, the laccolith model for crater modification also can constrain regional magma systems. In particular, it can model local magma column lengths and, with several craters, regional variations in magmatic activity (Wichman and Schultz 1995). Where driving pressures on Earth provide a direct estimate for crustal magma column lengths, however, the lunar models are complicated by higher relative magma densities.

On Earth, basaltic magmas are typically less dense than deep crustal rocks. Consequently, if overburden thickness is unchanged by uplift over an intrusion, $P_d = \Delta\rho g h$, where $h$ is the magma source depth beneath an intrusion and $\Delta\rho$ is the density contrast between the magma and the crustal section (Johnson and Pollard 1973). In contrast, mare basalt magmas on the Moon appear to be denser than the anorthositic lunar crust (Solomon 1975). Thus, any hydrostatic magma column in the lunar crust must be supported by an extension into the denser mantle, and the modeled magma pressures will reflect the lengths of both the crustal magma column and this deeper mantle ''root'' (Fig. 1).

Turning to our example at Taruntius, the inferred crustal thickness in this region is about 50 km (Bratt *et al.* 1985), and the laccolith model indicates a minimum intrusion depth of ~1–2 km. Thus, for an initial crater depth at Taruntius of ~2 km, the crustal column height ($h_c$ of Fig. 1) is roughly 46 km. Assuming average crust and mantle densities of 2800 and 3400 kg/m$^3$, respectively, this column length and a $P_d$ of 8.9 MPa then indicate a mantle column length ($d_s$) of 20.2 km and a total magma column length of ~66 km at Taruntius. Since $T_e$ gives a minimal value for the uplifted plate thickness (Pollard and Johnson 1973), these values are maximum estimates for the respective column lengths. Nevertheless, they seem to be fairly robust. Even if the intrusion depth is doubled, the indicated $d_s$ for Taruntius only decreases by ~600 m.

## CONCLUDING REMARKS

In addition to qualitatively explaining deformation in lunar floor-fractured craters (Wichman 1993), laccolith models for crater modification can help reveal the interaction of regional magmas with surface and subsurface crater

structures. Specifically, these models estimate subsurface intrusion dimensions, and they yield values for local magma pressure and for an effective plate thickness over the intrusion. The effective thickness, in turn, places strong constraints on the minimum depth of the intrusion, and a likely range of greater intrusion depths can also be modeled. Still, due to uncertainties in the stratigraphy of lunar crater floors, an absolute maximum depth cannot be derived. The derived magma pressures also constrain model magma column lengths beneath a crater, thereby revealing possible variations in magmatic activity during mare volcanism.

For the crater Taruntius, the model indicates emplacement of a laccolith 30 km wide and 1900 m thick. These dimensions imply a driving magma pressure of ~9 MPa (90 bar) in the intrusion and a flexural plate thickness of at least ~800 m over the intrusion. If changes in intrusion thickness over time and a (crudely) layered crater floor stratigraphy are allowed, likely intrusion depths range from ~1 to 5 km beneath the crater floor. Since intense impact brecciation on Earth apparently occurs at depths of <1/10 the crater diameter (Pohl *et al.* 1977, 1988), this depth range correlates well with the likely depths of intense brecciation at Taruntius (<6 km). If we also assume that the intrusion was fed by a hydrostatic magma column, the derived magma pressure and estimated crustal thickness imply a magma column at Taruntius roughly 65 km long and extending ~20 km beneath the crust/mantle boundary. This extension is presumed to be the thickness of magmas trapped at the base of the crust during crater modification.

## ACKNOWLEDGMENTS

We thank D. J. Roddy and M. R. Dence for their considered and insightful reviews of this manuscript.

## REFERENCES

Bratt, S. R., S. C. Solomon, J. W. Head, and C. H. Thurber 1985. The deep structure of lunar basins: Implications for basin formation and modification. *J. Geophys. Res.* **90,** 3049–3064.

Brennan, W. J. 1975. Modification of pre-mare impact craters by volcanism and tectonism. *Moon* **12,** 449–461.

Corry, C. E. 1988. *Laccoliths: Mechanisms of Emplacement and Growth.* Geol. Soc. Am. Special Paper **220**.

Danes, Z. F. 1965. Rebound processes in large craters. *Astrogeol. Stud. Annu. Prog. Rep. A (1964–1965)*, pp. 81–100.

Dence, M. R., R. A. F. Grieve, and P. B. Robertson 1977. Terrestrial structures: Principal characteristics and energy considerations. In *Impact and Explosion Cratering* (D. J. Roddy, R. O. Pepin, and R. B. Merrill, Eds.), pp. 247–275. Pergamon Press, New York.

Gilbert, G. K. 1877. *Report on the Geology of the Henry Mountains.* U.S. Geographical and Geological Survey of the Rocky Mountain Region, 170 pp.

Grieve, R. A. F., and M. J. Cintala 1992. An analysis of differential impact melt-crater scaling and implications for the terrestrial impact record. *Meteoritics* **27,** 526–538.

Hall, J. L., S. C. Solomon, and J. W. Head 1981. Lunar floor-fractured craters: Evidence for viscous relaxation of crater topography. *J. Geophys. Res.* **86,** 9537–9552.

Hulme, G. 1974. The interpretation of lava flow morphology. *Geophys. J R. Astron. Soc.* **39,** 361–383.

Jackson, M. D., and D. P. Pollard 1988. The laccolith-stock controversy: New results from the southern Henry Mountains, Utah. Geol. Soc. Am. Bull. **100,** 117–139.

Johnson, A. M., and D. P. Pollard 1973. Mechanics of growth of some laccolithic intrusions in the Henry Mountains, Utah. I. Field observations, Gilbert's model, physical properties and flow of magma. *Tectonophysics* **18,** 261–309.

Moore, H. J., and G. G. Schaber 1975. An estimate of the yield strength of the Imbrium flows. *Proc. Lunar Sci. Conf.* **6,** 101–118.

Moore, H. J., D. W. G. Arthur, and G. G. Schaber 1978. Yield strengths of flows on the Earth, Moon and Mars. *Proc. Lunar Planet. Sci. Conf.* **9,** 3351–3378.

Pike, R. J. 1980. Geometric interpretation of lunar craters. *U.S.G.S Prof. Pap.* **1046-C,** C1–C77.

Pohl, J., D. Stoffler, H. Gall, and K. Ernstson 1977. The Ries impact crater. In *Impact and Explosion Cratering* (D. J. Roddy, R. O. Pepin, and R. B. Merrill, Eds.), pp. 343–404. Pergamon Press, New York.

Pohl, J., A. Eckstaller, and P. B. Robertson 1988. Gravity and magnetic investigations in the Haughton impact structure, Devon Island, Canada. *Meteoritics* **23,** 235–238.

Pollard, D. P., and A. M. Johnson 1973. Mechanics of growth of some laccolithic intrusions in the Henry Mountains, Utah. ll. Bending and failure of overburden layers and sill formation. *Tectonophysics* **18,** 311–354.

Schultz, P. H. 1972. *A Preliminary Morphologic Study of Lunar Surface Features.* Ph.D. Thesis, University of Texas at Austin.

Schultz, P. H. 1976. Floor-fractured lunar craters. *Moon* **15,** 241–273.

Solomon, S. C. 1975. Mare volcanism and lunar crustal structure. *Proc. Lunar Sci. Conf.* **6,** 1021–1042.

Whitford-Stark, J. L. 1974. Internal origin for lunar rilled craters and the maria? *Nature* **248,** 573–575.

Wichman, R. W. 1993. *Post-impact Modification of Craters and Multiring Basins on the Earth and Moon by Volcanism and Lithospheric Failure.* Ph.D. Thesis, Brown Univ., Providence, RI.

Wichman, R. W., and P. H. Schultz 1995. Floor-fractured craters in Mare Smythii and west of Oceanus Procellarum: Implications of crater modification by viscous relaxation and igneous intrusion models. *J. Geophys. Res.* **100,** 21,201–21,218.

Young, R. A. 1972. Lunar volcanism: Fracture patterns and rilles in marginal pre-mare craters. *Apollo 16 Prelim. Sci. Rep., NASA SP-315,* 29-89–29-90.